

Chapter 2

Application of Laser-Induced Fluorescence Technique in Internal Combustion Engine Investigations



Tushar Kakkar, Ashutosh Jena, and Avinash Kumar Agarwal

Abstract Laser diagnostic techniques have evolved as a pioneering tool for understanding the combustion and fluid dynamics in internal combustion (IC) engines. These are non-intrusive techniques, which provide fundamental insights about the in-cylinder processes such as spray characteristics, fuel-air mixing, combustion, pollutant formation, etc. without affecting/altering the underlying physics. This chapter is based on one such laser diagnostic technique namely ‘laser-induced fluorescence (LIF)’, which is capable of imaging the temperature-field and in situ species concentration during combustion. This chapter discusses a brief overview of optical diagnostics techniques, fundamentals of LIF, design, and development, current status and future trends for the application of this technology in IC engine research. This chapter also includes a comprehensive literature review of the applications of LIF in combustion investigations with a special emphasis on IC engines. Several examples and case studies have also been included in this chapter for a better understanding.

Keywords Laser-induced fluorescence · Optical diagnostics · IC engines · Equivalence ratio · Emission formation

2.1 Introduction

In the last few decades, advanced combustion technologies have been developed to reduce the formation of harmful pollutants in the engine along with an optimum trade-off between engine-out emissions and engine performance. These advanced combustion techniques are based on optimum engine control parameters as well as a selection of advanced control strategies such as fuel injection parameters, intake air pressure and temperature, etc. In many studies, it has already been proven that the in-cylinder temperature/pressure and equivalence ratio of the fuel–air mixture affect the quality of combustion. These physical quantities together control the onset

T. Kakkar · A. Jena · A. K. Agarwal (✉)
Engine Research Laboratory, Department of Mechanical Engineering, Indian Institute of Technology Kanpur, Kanpur 208016, India
e-mail: akag@iitk.ac.in

© The Author(s), under exclusive license to Springer Nature Singapore Pte Ltd. 2021
A. P. Singh and A. K. Agarwal (eds.), *Novel Internal Combustion Engine Technologies for Performance Improvement and Emission Reduction*, Energy, Environment, and Sustainability, https://doi.org/10.1007/978-981-16-1582-5_2

of ignition, flame propagation, and combustion stability, which are important for optimum engine design. Computational fluid dynamics (CFD) analysis has evolved as an important tool for engine development; however, the use of CFD models for successful prediction of complicated combustion phenomenon relies heavily on the generation of accurate experimental data for model validation. Therefore, reliable measurement of in-cylinder processes and temperature distribution in the engine hold the key for futuristic emission compliant high-performance internal combustion (IC) engines.

For this purpose, several optical diagnostic tools have been developed to understand the in-cylinder physics/processes, in which several laser diagnostic techniques such as Laser Rayleigh Scattering (LRS), Raman scattering, Coherent Anti-stokes Raman Scattering (CARS), etc. are used for in-cylinder temperature and species concentration measurements. Laser-induced fluorescence (LIF) is a well-established optical diagnostics technique for in situ measurement of species concentrations and temperature measurement during combustion. It produces relatively stronger signal intensity with high spatial resolution compared to other techniques. In this technique, the emission spectra are red-shifted from absorption, hence, provide relatively easier discrimination of the results. This technique is important for both quantitative and qualitative analyses of different species up to sub-ppm level. This chapter discusses different aspects of LIF technique such as the basic principle of LIF technique, method of measurements, application of LIF in different engine technologies, etc. Several case studies have also been discussed for a better understanding of this technique and its capabilities.

2.2 LIF-Based Diagnostics

2.2.1 Basic Principle

LIF works on the basis of excitation of target species molecules from lower energy state to higher energy state, which emit fluorescence during spontaneous de-excitation. The emitted photon wavelength by the excited species is different from the wavelength of the exciting source. The excitation wavelength coincides with the absorption wavelength. The amount of energy absorbed and the amount of energy emitted depend on the particular species getting excited.

Excited species are often involved in multiple energy interactions, in which a further excitation to a higher energy state is possible due to excitation by absorption of an additional photon. The molecules also undergo inelastic collisions with other molecules. This phenomenon alters the electronic energy of the molecules and is known as quenching. Quenching affects the fluorescence quantum yield (ϕ), which is defined as the ratio of photons emitted during emission to photons absorbed during excitation. Therefore, by analysing the radiation spectra, desired information such as temperature and concentration of species can be obtained. Figure 2.1 shows the

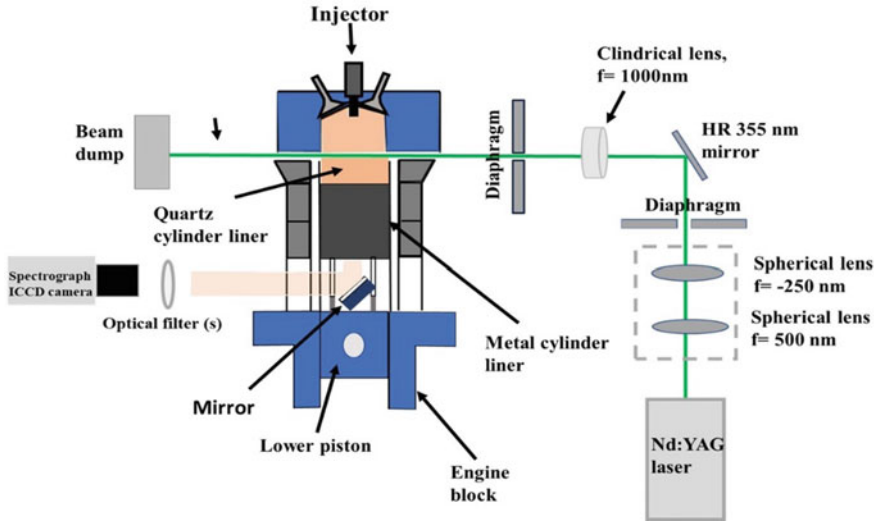


Fig. 2.1 Schematic of the LIF experimental setup

schematic of a LIF experimental setup in an optical engine, in which the laser beam is converted into a thin light sheet with the help of light-sheet optics. The engine cylinder liner is modified to provide laser access to the cylinder. The LIF signals are captured by the high-speed camera using appropriate filters. The piston is also provided with an optical window for enabling the camera to capture the fluorescence signals.

2.2.2 Tracers

In LIF technique, single component species having definite spectral behaviour are used as tracer to measure the local distribution of physical quantities like temperature, concentration, etc. Selection of suitable tracers is important for precise measurement in the experimental domain. The signal yield for a specific tracer depends on the environment under study. This sub-section describes the photo-physical aspects and associated challenges for tracers in the LIF studies.

2.2.2.1 Ideal Tracer

Stimulation of suitable wavelength excites the species from one electronic/vibrational state to another. Such species are known as the tracer species, which may be naturally present or sometimes need to be introduced. While natural tracers are inherent to fuels, foreign tracers are mixed with the fuel in required proportions. Ideally, the

tracer should have exactly similar properties to that of the parent fuel. It should behave like a replacement for the components in a multi-component fuel having different aspects of physical properties such as evaporation, diffusivity, etc. An ideal tracer should emit fluorescence proportional to its concentration. The tracer must not induce any perturbation to the original system under investigation. It must not affect the combustion kinetics. Properties of tracer species should be invariant with ambient conditions such as temperature and pressure. However, it is very unlikely that any tracer will closely follow the requirements of an ideal tracer. Temperature and pressure dependencies are inevitable for all tracer species. Next sub-section deals with a few examples of different natural and foreign tracers, and their limitation. This sub-section gives more emphasis to toluene, which is the most widely used tracer in LIF studies.

2.2.2.2 Tracers in Practical Applications

During the combustion of fuels, a number of intermediate species and by-products are formed. However, the major part of intermediate species is saturated hydrocarbons, which do not generate any LIF signal in the required range of the spectrum. There are few species such as aromatic hydrocarbons present in fuels, which emit fluorescence signals and act as natural tracers. Similarly, formaldehyde, an intermediate species formed during combustion in the low-temperature regime, is also capable of producing fluorescence signals. It gets further oxidized and vanishes, when the local temperature rises. The Presence of formaldehyde marks a low-temperature region in the combustion chamber and its measurement has been demonstrated elsewhere as well (Hildingsson et al. 2005; Schießl and Maas 2003). By fuel tracer LIF approach, it is confirmed that the dark pockets are lower temperature regimes, where intermediate reactions are yet to start. Since formation of intermediates are highly temperature-sensitive, the temperature variation can be extracted from the fluctuations of the concentration field of these species. For this, first, it is necessary to investigate a correlation between temperature and concentration of intermediate species. Schießl and Maas (2003) observed a strong relationship between temperature and concentration of formaldehyde, which indicates the possibilities of detecting temperature fluctuations by means of measuring spatial changes in $[H_2CO]$. This study demonstrated that the fluctuations in the amplitude of concentrations can be mapped into a temperature interval via the correlation $[H_2CO] = f(T)$. Commercial fuels consist of several species, which act as a natural tracer, however, they are not helpful in the quantitative analysis. Physical properties of such species present in commercial fuels vary with varying ambient conditions, leading to an ambiguity in signal detection. However, some fuels do not emit detectable fluorescence. Peterson et al. (2015) found that iso-octane vapours in the intake flow did not yield any fluorescence. In such conditions, foreign tracers such as rhodamine, ketones etc. are used in a non-fluorescing base liquid (Schulz and Sick 2005). For quantitative analysis, spectroscopic grade fuel should be used for the best results. Thallium chloride and indium chloride can also be used for qualitative temperature analysis of burned gases. An

extensive study of a variety of tracers was carried out by Schulz and Sick (2005), in which ketones were suggested as one of the best tracers for LIF. LIF signal obtained from organic molecules like ketones or toluene depends strongly on temperature, which is helpful for simultaneous measurements of in situ species concentration and temperature. Fujikawa et al. (2006) used 3-pentanone as a fluorescence tracer for the LIF technique. They found that the quantum efficiencies of ketones are 1/10th or less than that of aromatic hydrocarbon molecules. Therefore, aromatic hydrocarbons such as toluene are often preferred as a foreign tracer. They demonstrated that toluene (5% w/w) has a comparable intensity for 3-pentanone; however, the quantum efficiency of toluene was relatively higher than ketones. A temperature-dependent shift in toluene emission spectra offers the simplicity of using single line extraction (excitation with a single laser of a particular wavelength), which reduces the experimental cost and complexity (Peterson et al. 2013). 3-pentanone and toluene are also extensively used for experiments under high temperature and pressure conditions. Therefore, 3-pentanone and toluene can also be used as a primary LIF tracer in IC engines. In IC engine experiments, strong temperature sensitivity of toluene also provides important information about the flow structure, however, 3-pentanone provides only noteworthy measurements compared to toluene (Peterson et al. 2015; Gamba et al. 2015). Toluene is compatible with most commercial fuels (iso-octane and n-heptane), which have components similar to toluene (Gessenhardt et al. 2015; Kaiser et al. 2013). Although, high-speed toluene LIF thermometry measurements are accurate and provide important information about the transport of gas temperature, improved precision is still essential to make this technique more effective (Peterson et al. 2013). In most studies, one colour detection technique was used in toluene LIF due to superior temperature sensitivity and precision, however, sometimes, one colour detection technique results in inaccuracy due to local LIF signal variations caused by local toluene mixture heterogeneity (Gamba et al. 2015). Under such conditions, two-colour detection technique is preferred in toluene LIF thermometry measurements. In two-colour toluene thermometry, modest sensitivity and strong quenching of toluene LIF by oxygen reduce the signals in the air (in fired engine operation conditions) with minimum variation in the colour ratio. In some studies, nitrogen addition resolved quenching issues in non-reacting environment (Gessenhardt et al. 2015; Peterson et al. 2014). There are few other aspects such as pressure effect (air/fuel) of toluene, which make its application challenging in LIF measurements (Kaiser et al. 2013).

2.2.3 Material for Optical Access

Detailed information related to optical access is an important aspect, which is by and large missing in the previous studies. In most studies, quartz is the most widely used material for providing optical access into an engine as well as in the constant volume combustion chamber (CVCC) (Schießl and Maas 2003; Peterson et al. 2013; Zhang et al. 2019; Haessler et al. 2012; Li et al. 2013; Scott et al. 2017; Chen et al. 2019).

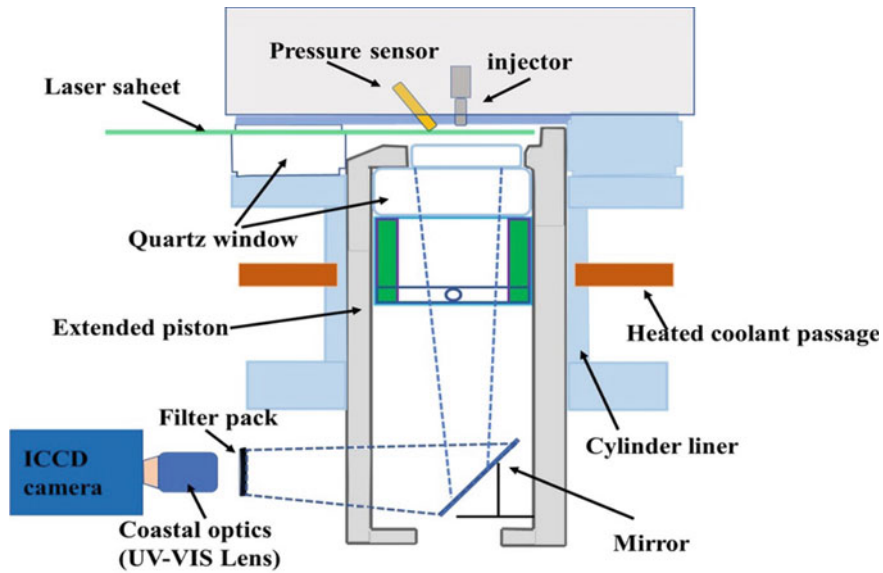


Fig. 2.2 Schematic of an engine with optical access

In last few years, the use of quartz as a suitable material for optical access into the IC engine combustion chamber has increased rapidly due to the adaptation of different laser diagnostic techniques (Fig. 2.2).

There are few other materials such as sapphire, and fused silica which are used for providing the optical access in to metallic engines. Tensile strength of sapphire is comparable to cast iron. It has a Mohs hardness of 9 with favourable mechanical properties, which provides abrasion resistance (Miles 2014). Sapphire has the ability to retain its strength at a very high temperature. Thermal expansion coefficient of sapphire is appropriate to form an interface boundary with stainless steel. This is a unique feature, which reduces thermal stress/thermal shock at the interface of the two materials. Figure 2.3 depicts that a large thermal strain can change the shape of the material, which alters the laser path. This results in a serious issue related to laser focusing and data acquisition (Miles 2014). Relatively, inferior optical property of sapphire compared to quartz is, however, another issue. It has a much higher refractive index, which leads to a high image distortion with a curved sapphire window. Sapphire has a high mass density, which is almost twice of quartz. This further adds to the balancing issue of the elongated piston when used as a piston window material. Itani et al. (2015) demonstrated the use of sapphire in high-pressure, high-temperature, pre-combustion vessel. They used two cylindrical sapphire windows (with a field of view $85 \times 85 \text{ mm}^2$) on opposite sides of the vessel. This vessel has two more windows of $65 \times 10 \text{ mm}^2$ for providing access to laser beams.

Fused silica has also been used in many optical studies, where the thickness of fused silica window ranges between 3 to 70 mm, depending on ambient requirements

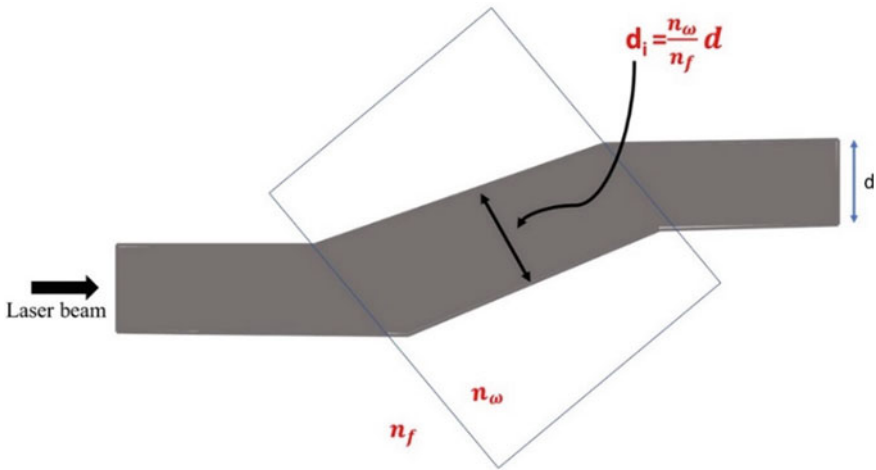


Fig. 2.3 Effect of thermal stresses on optical material shape

(Fujikawa et al. 2006; Li et al. 2006; Burkert et al. 2013; Lind et al. 2017). In order to protect whole optical assembly against the cylinder pressure, Gessenhardt et al. (2015) used fused silica as window material with an arrangement of thin titanium bushing with a press-fit sapphire window of 2.7 mm thickness for pressure sealing. Burkert et al. (2013) also used a high-pressure stainless steel cell, equipped with fused silica windows. These windows were capable of sustaining up to 100 bar pressure and 1000 K temperature.

2.2.4 Laser

Nd:YAG laser with a wavelength in the range 266–355 nm is the most used laser for LIF investigations (Peterson et al. 2013, 2014, 2015; Gessenhardt et al. 2015; Scott et al. 2017; Chen et al. 2019; Lind et al. 2017; Kranz and Kaiser 2019; Strozzi et al. 2019). In few studies, many other types of lasers such as XeCl laser (Schießl and Maas 2003), XeF laser (Burkert et al. 2002), etc. have been used. Fujikawa et al. (2006) carried out experiments using three different lasers namely: KrF excimer laser (248 nm), the fourth harmonic of Nd:YAG laser (266 nm), and the second harmonic of a dye laser. Kaiser et al. (2013) compared the performance of KrF excimer laser with Nd:YAG laser. They reported that KrF excimer laser excited at 248 nm and resulted in more unbiased detection due to different excitation wavelengths compared to fluorescence. KrF excimer laser resulted in 2–3 times longer pulse length compared to Nd:YAG laser. Bessler et al. (2001) and Schulz et al. (1995) also used KrF excimer

laser and reported relatively higher gain of KrF excimer laser compared to Nd:YAG laser.

2.3 Applications of LIF

2.3.1 Concentration and Temperature Determination

Concentration measurement in isothermal condition

For quantitative measurements of in situ species concentration and temperature in an IC engine, in-cylinder pressure can be taken to be constant throughout the interrogation volume. The pressure data can be easily obtained from a pressure transducer, which can be used as a reference during calibration. Moreover, under some conditions, the in-cylinder temperature can be approximated as being spatially invariant. Average temperature can be calculated with the knowledge of pressure, assuming adiabatic compression. This would make the measurement of species concentration quite straight forward. Under the isobaric and isothermal conditions, LIF intensity is directly proportional to the species concentration. During an experiment, unknown concentration (n_{exp}) can be determined by using the following equation.

$$n_{\text{exp}} = n_{\text{cal}} (S_{\text{exp}} / S_{\text{cal}}) \quad (2.1)$$

where, S_{exp} is the signal measured during the experiment. The fluorescence signal (S_{cal}) is obtained for a known concentration (n_{cal}). However, this case is not often realized. During transient mixing and evaporation of fuel, spatial gradients in temperature as well as concentration fields exist. Therefore, temperature measurements are essential and primary to correct the fuel concentration measurements.

Temperature measurement

The fluorescence signal intensity is given by Thurber (1999):

$$S_{\text{fl}} = \eta \cdot E \cdot r_{\text{Tracer}} \cdot \sigma(\lambda_{\text{ece}}, T) \cdot \phi(\lambda_{\text{ece}}, p, T) \quad (2.2)$$

where

- η = optical efficiency factor,
- E = laser pulse energy,
- r_{Tracer} = tracer partial density,
- λ_{ece} = excitation wavelength,
- σ = absorption cross-section, and
- ϕ = fluorescence quantum yield.

For a certain optical setup and tracer, S_{fl} is a function of pressure, temperature and concentration of tracer only. Thus, for known number density and pressure (isothermal, isobaric conditions), calibration can be done to obtain the temperature.

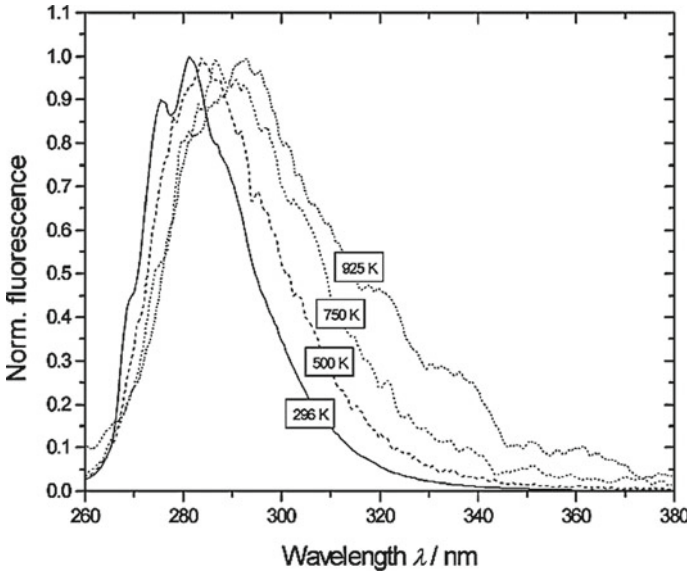


Fig. 2.4 Toluene fluorescence spectra variations with temperature (Koban et al. 2004)

Figure 2.4 depicts the variations in fluorescence yield with temperature for toluene. Calibration was done with 248 nm excitation and nitrogen bath gas pressure of 1 bar for a temperature range of 300–950 K (Koban et al. 2004). However, in many applications, the number density is unknown due to heterogeneous distribution. In such a case, the temperature-dependent red-shift of tracer spectrum can be exploited. Figure 2.4 shows the emission spectra of toluene for 248 nm excitation and 1 bar pressure. The peak of the spectra moves rightwards as the temperature increases. For a given temperature, fluorescence signals at two different wavelengths in the spectrum are detected. The ratio of intensities is determined to eliminate the requirement of number density (r_{Tracer}). Calibration is done at multiple temperature points (at constant pressure) and final calibration curve is obtained by curve fitting. Similarly, multiple calibration curves are required for the measurements at different crank angle positions in the engine because in-cylinder pressure varies with crank angle.

$$\frac{(S_f)_{\lambda 1}}{(S_f)_{\lambda 2}} = f(T) \quad (3)$$

Figure 2.5 shows the signal ratio for the calibration of toluene LIF with 266 nm excitation. The signals were obtained at 280 nm and 335 nm respectively (Koban et al. 2004). This method of temperature measurement with single-colour excitation and two-colour detection is known as ‘two-colour detection’ technique.

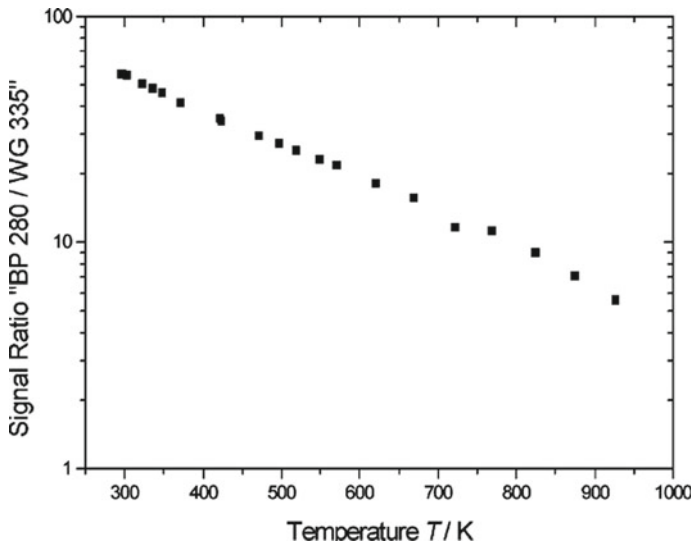


Fig. 2.5 Signal ratio of toluene for different temperatures (Koban et al. 2004)

For in-cylinder measurements, the LIF signal distribution is obtained for a particular crank angle. The data are then normalized and converted to temperature distribution by comparing the signal ratio at each pixel with the calibration curve. Once the temperature is determined from the calibration curve, the unknown concentration can be obtained by putting the value of temperature in the Eq. 2.2. The calibration is preferably done in the same setup to obtain a high degree of accuracy. Table 2.1 documents a chronicle of different studies related to temperature and concentration measurements using LIF technique in engines and CVCCs.

2.4 LIF Case Studies

This section discusses various applications of LIF studies in different engines and CVCCs. A brief summary on the experimental methods and experimental setup details have been provided along with important results of a large number of experimental studies.

Table 2.1 Summary of LIF studies for different applications

Engine	Combustion technology	Fuel with tracer percentage	Physical quantity measured	References
CI	Conventional CI	Heptane with iso-octane and toluene (65%, 25%, 10% v/v)	Temperature	Hildingsson et al. (2005)
		Heptane with ketone (2% v/v)	Temperature	Schulz et al. (1995)
		Diesel and n-heptane with CH ₂ O	Temperature	Donkerbroek et al. (2010)
			Species concentration	Donkerbroek et al. (2010)
		Diesel with natural occurring tracer (formaldehyde, OH, NO)	Temperature	Verbiezen et al. (2007)
	PRF77 and acetone (10% v/v)	Species concentration	Shi et al. (2020)	
		Temperature	Shi et al. (2020)	
	HCCI (CAI)	Nitrogen with iso-octane and toluene (50-50% v/v)	Temperature	Kaiser et al. (2013)
			Temperature	Nygren et al. (2002)
		Ethanol with acetone (10% v)	Species concentration	Nygren et al. (2002)
			Species concentration	Li et al. (2013), Zhao (2004)
	n-heptane with naturally occur tracer (CH ₂ O, OH)	Temperature	Brackmann et al. (2003)	
		Species concentration	Brackmann et al. (2003), Schrewe and Gandhi (2007)	
	RCCI	Iso-octane with n-heptane and toluene (70%, 30% and 1% v/v)	Temperature	Tang et al. (2017)
			Temperature	Tang et al. (2020)
Polyoxymethylene dimethyl ethers, iso-octane, n-heptane with cetane and (natural tracer OH)		Species concentration	Tang et al. (2020)	
PCC/PCCI/GCI/PPC	Iso-octane with n-heptane and toluene (70%, 30% and 1% v/v)	Temperature	Tang et al. (2017)	

(continued)

Table 2.1 (continued)

Engine	Combustion technology	Fuel with tracer percentage	Physical quantity measured	References
		PRF70 fuel and toluene (1% v)	Temperature	Raman et al. (2020)
			Species concentration	Raman et al. (2020)
SI	GDI/DISI	Toluene (2.75% v)	Temperature	Peterson et al. (2015), Peterson et al. (2013), Peterson et al. (2014)
			Species concentration	Scott et al. (2017)
		Iso-octane with toluene (7-3% v/v)	Species concentration	Scott et al. (2017)
		Formaldehyde (H ₂ CO)	Temperature	Schießl and Maas (2003) Lachaux and Musculus (2007)
			Species concentration	Schießl and Maas (2003), Lachaux and Musculus (2007)
		NO	Temperature	Schulz et al. (1995)
		n-pentane, iso-octane, n-undecane (36%, 46%, 18% v/v) with tracer (DFB (0.02%), 1MN (0.1%), ANI (0.4))	Temperature	Kranz and Kaiser (2019)
		Iso-octane with natural occurring tracer (CH ₂ O)	Temperature	Brackmann et al. (2003)
			Species concentration	Bessler et al. (2001), Brackmann et al. (2003)
		Gasoline with biacetyl	Species concentration	Deschamps et al. (1996)
Gasoline surrogate + ethanol (20% and 85%) with tracer	Species concentration	Bardi et al. (2019)		
Iso-octane with triethylamine (TEA) and acetone (0.25% and 2.5% v/v)	Temperature	Lind et al. (2015)		
	Species concentration	Lind et al. (2015)		

(continued)

Table 2.1 (continued)

Engine	Combustion technology	Fuel with tracer percentage	Physical quantity measured	References
		Butanes with Isopentanes and acetone (5% v/v)	Temperature	Williams et al. (2010)
			Species concentration	Williams et al. (2010)
		Iso-octane with n-octane and toluene (2% v/v)	Temperature	Williams et al. (2010)
			Species concentration	Williams et al. (2010)
		Iso-dodecane with n-Decanes and TMB (2% v/v)	Temperature	Williams et al. (2010)
			Species concentration	Williams et al. (2010)
		Iso-pentane, iso-octane with n-nonane (20%, 70%, 10% v/v) and tracer foxylene/acetone (1:5, v:v), toluene/acetone (1:2, v:v), p-xylene/3-pentanone(1:5 v:v)	Temperature	Krämer et al. (1998)
	Species concentration		Krämer et al. (1998)	
	DMF with MF and OH	Species concentration	Ma et al. (2014)	
	Oil and pyrromethene 567(0.1 mmol/L)	Temperature	Cheong et al. (2020)	
	PFI	Iso-octane with toluene (4:1 v/v)	Temperature	Gessenhardt et al. (2015)
		Iso-octane with toluene (5% v)	Temperature	Fujikawa et al. (2006)
		Hexane with 3-pentanone (25%v) and iso-octane with DMA (10%)	Species concentration	Li et al. (2006)
Iso-octane with natural occurring tracer		Temperature	Peterson et al. (2019)	
	Species concentration	Peterson et al. (2019)		
CVCC	Calibration cell/combustion chamber shell	GTL-diesel with 1-MN (0.5%v)	Temperature	Lind et al. (2017)
		Formaldehyde (H ₂ CO)	Temperature	Haessler et al. (2012), Burkert et al. (2002)
		Nitrogen with acetone (23% v)	Species concentration	Zhang et al.(2019)

(continued)

Table 2.1 (continued)

Engine	Combustion technology	Fuel with tracer percentage	Physical quantity measured	References
		Gasoline with p-Difluorobenzene and 1-methylnaphthalene (0.02% and 0.1%)	Temperature	Itani et al. (2015)
		GTL-diesel with natural tracer	Species concentration	Burkert et al. (2013)
		n-heptane with natural tracer	Temperature	Ottenwalder et al. (2018)
			Species concentration	Ottenwalder et al. (2018)
		Gasoline with ethanol (20% and 85 v/v) and p-difluorobenzene and 1-methylnaphtalene	Temperature	Cordier et al. (2020)
			Species concentration	Cordier et al. (2020)
N-dodecane with Naphthalene and TMPD (90%, 9% and 1% v/v)	Temperature	Chen et al. (2019)		
Misc.	Jets in supersonic cross -flow	Nitrogen with toluene (0.5% v)	Temperature	Gamba et al. (2015)
	Reacting flows	OH	Temperature	Malmqvist et al. (2016)
			Species concentration	Malmqvist et al. (2016)
	Corona discharge	O ₂ , N ₂ with NO	Species concentration	Shen et al. (2012)
	LIF in methane/air Flames	Propane	Species concentration	Bessler et al. (2002)
	Turbulent premixed conical flames	OH radical	Species concentration	Deschamps et al. (1996)
	Study on mixing phenomenon inside reactor down-comer	Salted tracer concentration	Species concentration	Zhang et al. (2019)
	Imaging of methyl radical (CH ₃) in premixed methane/air flames	Methane and CH	Species concentration	Li et al. (2017)
	Temperature measurements in RCM	Iso-octane and anisole	Temperature	Tran et al. (2015)
Magnetic resonance concentration measurements	De-aerated water with copper sulphate	Temperature	Banko et al. (2020)	

(continued)

Table 2.1 (continued)

Engine	Combustion technology	Fuel with tracer percentage	Physical quantity measured	References
	Laminar premixed low-pressure flame experiments	OH	Species concentration	Schmitt et al. (2020)
	Micro-explosion of emulsion drops	Oil with water and fluorescein (250 and 300 mg/L) and rhodamine B(25,50,100 mg/L)	Temperature	Omar et al. (2020)
			Species concentration	Omar et al. (2020)
	Effects of lubricant oil film adhering on cylinder wall on the post fuel impingement and adhesion of spray penetration, wall impingement behaviour	Oil and rhodamine-B (0.1% v/v)	Temperature	Shibata et al. (2020)
		JIS K2204 (Japanese diesel) with ethanol (5%v/v) and rhodamine-B (0.05%)	Temperature	Shibata et al. (2020)
	Turbulent buoyant jet in the self-similar region	Rhodamine-6G	Temperature	Qin et al. (2020)
			Species concentration	Qin et al. (2020)
	Single-shot 3D flame diagnostic based on volumetric LIF	CH	Temperature	Ma et al. (2017)
			Species concentration	Ma et al. (2017)
	Single-shot measurements in turbulent flows	Nitrogen and I ₂ (iodine crystals)	Temperature	Wu et al. (2015)
			Species concentration	Wu et al. (2015)
	Pyrolysis of toluene behind reflected shock waves	Argon and toluene (0.1–2% v/v)	Temperature	Zabeti et al. (2015)

2.4.1 A Case Study of Thermal Stratification in HCCI Engine

Despite having an immense potential of HCCI combustion engines in cutting-down the emissions to meet future emission norms, there are several hurdles in the commercialization of HCCI engine technology. Cycle-to-cycle variations is one such major hurdle, which has been reported by many researchers. Variations in the local temperature field from cycle-to-cycle is one of the main reasons for cyclic variations in HCCI combustion engines. LIF imaging of homogenous toluene seeded intake charge was used to study the fluctuation of the temperature field over cycle averaged mean

temperature field (Kaiser et al. 2013). The experimental setup for this study is shown in Fig. 2.6. Other important experimental details are given in Tables 2.2 and 2.3.

A single-cylinder engine was used in this experiment, which consisted of a pent-roof four-valve cylinder head and a flat top piston with an optical window. Toluene was seeded through the intake to achieve homogenous mixing with the inlet flow. This was essential for precise calibration and measurement of the temperature field. Toluene has properties similar to iso-octane and n-heptane. Toluene was mixed with iso-octane fuel (50% v/v) and was then premixed with nitrogen gas using an injector (hollow type) working at a fuel injection pressure of 120 bar, and then introduced

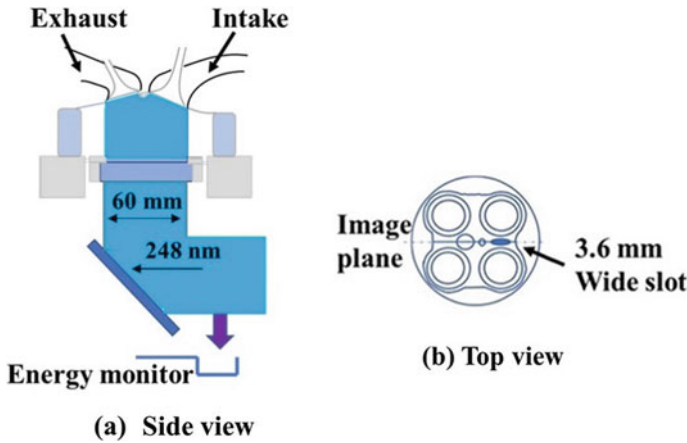


Fig. 2.6 Experimental setup

Table 2.2 Engine geometry and experimental conditions (Kaiser et al. 2013)

Bore	84 mm
Stroke	90 mm
Displacement	499 cm ³
Geometric compression ratio	10
Speed	2000 rpm
Intake pressure and gas	1 bar, nitrogen

Table 2.3 Experimental error sources in LIF measurements (Kaiser et al. 2013)

Error source	Relative signal RMS [%]	
	At BDC	At TDC
Camera noise	0.25	1.1
Energy fluctuations	1.4	1.4
Mode fluctuations	3.5	3.5
Total RMS error [% signal]	3.8	3.9
Total RMS temperature error [K]	1.6	4.0

into the combustion chamber. The KrF excimer laser (248 nm) was used for the excitation.

1 mm thick laser sheet was guided vertically in an upwards direction opposite to the pent-roof cylinder head through the mirror in the extended piston (as shown in Fig. 2.6) and the signal pulse measurement was done by diverting a fraction of laser sheet onto a photo-diode. A CCD camera was employed for signal detection. A fused silica window ring spanning 25 mm from the cylinder head was used to gain optical access.

Figure 2.7 shows the variations in temperature distribution during the compression stroke. The fluctuations shown are relative to the mean bulk temperature measured at each piston position during the compression stroke. Such distribution could have resulted from the inhomogeneous mixing of the charge. It was observed that variations increased as the piston moved closer to the cylinder head. However, no significant gradient in temperature was seen near the central region. Observed fluctuations were located near the wall boundaries. Observed variations at -180°CA could have resulted from inhomogeneity in the mixing of fuel and air. The location of injector in the port could be crucial in this aspect. During compression, temperature fields become more uniform because of turbulence. Hence variations at TDC have no relation with those present during the intake.

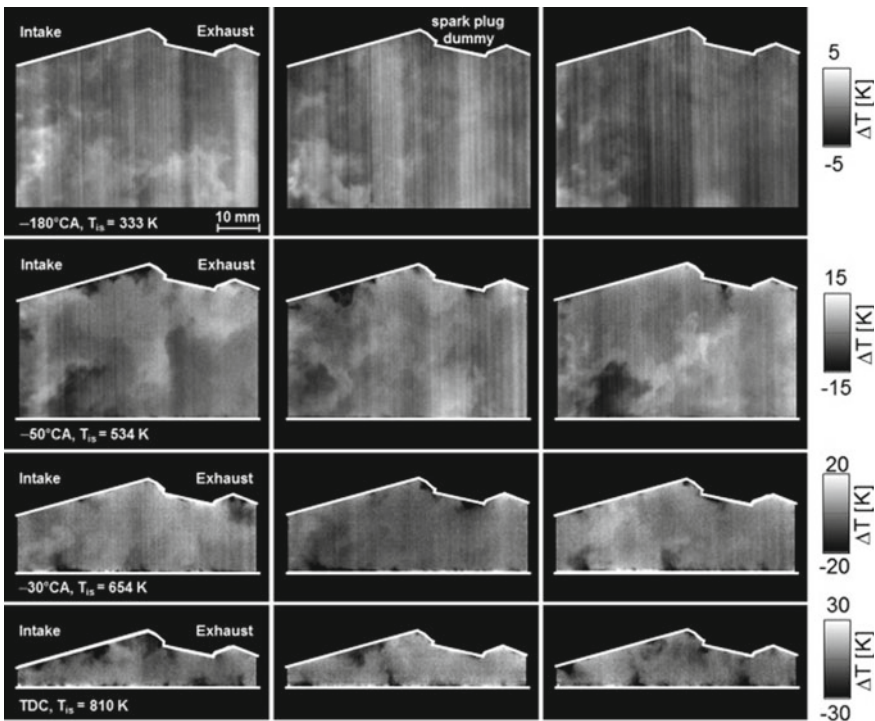


Fig. 2.7 Transition in the spatial structures (Kaiser et al. 2013)

2.4.2 A Case Study of Diesel Spray Diagnostics

The temperature and concentration field of fuel spray are vital to understand fuel–air mixing and ignition delay related phenomenon in CI engines. CVSC and CVCC have emerged as excellent alternatives to optical engines to extract important information about fuel spray and combustion respectively. Lind et al. (Lind et al. 2017) used 1- methyl naphthalene (1-MN) as tracer to understand fuel–air mixing of diesel spray in a high-temperature ambient environment. A study was carried out in a CVCC and it was reported as a pioneering research to employ PLIF concept for such analysis. Schematic of the experimental setup is shown in Fig. 2.8 and important details of spray chamber, operating parameters, etc. are provided in Table 2.4. For spectral fluorescence characterization, fluorescence spectrum was detected by the spectrograph with a blaze wavelength of 300 nm and 300 line/mm. Signal ratio calibration was done through two intensified charge-coupled device (ICCD) cameras. Light scattered from the laser was blocked by providing a 266 nm long-pass filter.

The chamber used in this study had five optical windows made of fused silica. Nd:YAG laser (266 nm, 10 Hz, 16 mJ/cm³) was used for excitation. Two-colour detection method was adopted for measurement. The effect of laser power fluctuations was taken care during image post-processing. Signals were acquired normal to the plane of illumination. A 50/50 beam splitter enabled imaging using two ICCD

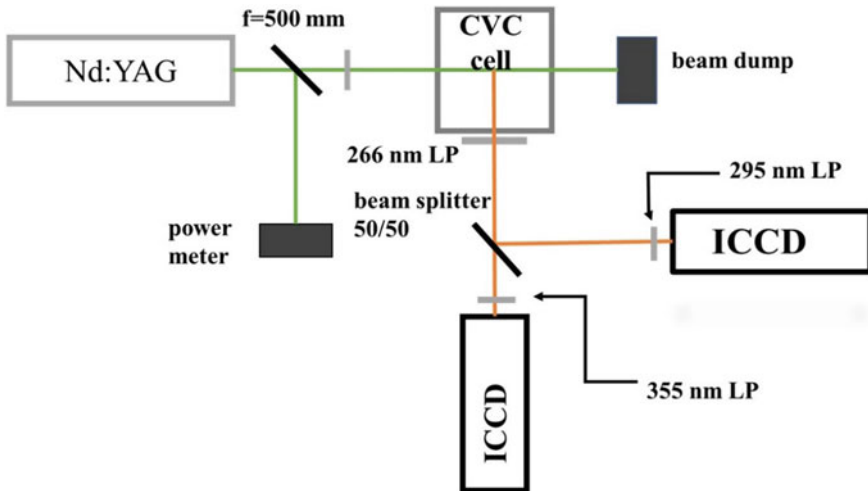


Fig. 2.8 Experiment setup for diesel spray diagnostics using LIF

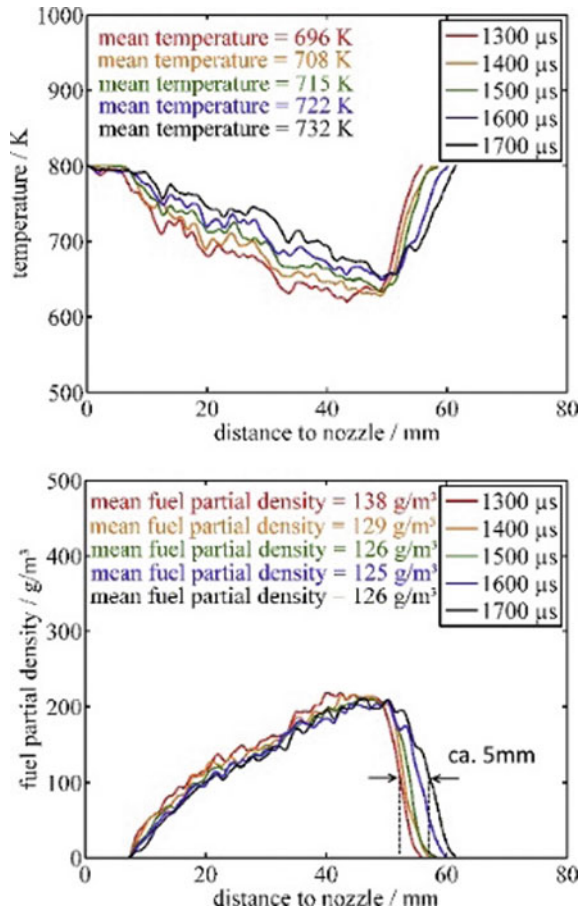
Table 2.4 Spray chamber operating conditions for LIF investigations (Lind et al. 2017)

	Maximum capacity	Operating condition
Temperature	1000 K	800 K
Pressure	10 MPa	5 MPa

cameras, as shown in the schematic. Signals were acquired for 295 nm and 355 nm using long-pass filters. CVCC was continuously scavenged with nitrogen gas. Non-fluorescent GTL diesel with added tracer (0.5% v/v) was injected using a 3-hole injector.

Figure 2.9 depicts pulse-averaged temperature variations along the spray axis. It can be observed that the temperature decreased with increasing distance from the nozzle exit up to 50 mm and then increased. Reduction in temperature was attributed to evaporative cooling of the spray, which was also supported by increasing density with distance from the nozzle exit. Increased level of turbulence at injector tip promoted turbulent mixing, leading to increased heat transfer. Figure 2.10 shows pulse-to-pulse variations in the temperature and density distributions. Results showed that the spray boundary temperature approached ambient temperature due to hot gas entrainment; however, core region did not show significant variations. This can also be seen in density distributions, where core density was significantly higher than the density at the spray boundary.

Fig. 2.9 Variations of temperature (top) and density with axial distance from nozzle (Lind et al. 2017)



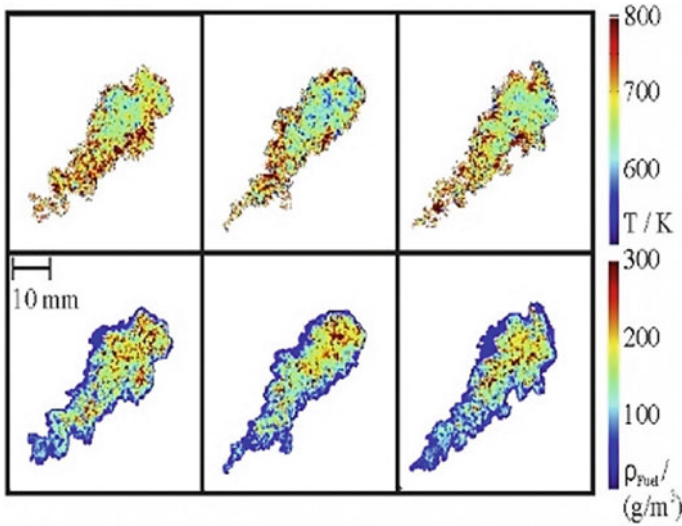


Fig. 2.10 Temperature and density distribution of diesel spray (Lind et al. 2017)

2.4.3 *A Case Study on High-Speed Toluene-LIF Thermometry with Two-Colour Detection Scheme in a GDI Engine*

Spray-induced evaporative cooling in GDI engine leads to a temperature stratification in the combustion chamber. During stratified mode operation, thermal stratification plays a major role in determining flame development and pollutant formation at retarded fuel injection. Therefore, it is crucial to understand the effect of spray on the temperature field. Simultaneous analysis of spray morphology and air motion can provide deep insights into this phenomenon. Therefore, a detailed study was carried out, in which spray characteristics were obtained by Mie scattering and flow dynamics was investigated using PIV (Peterson et al. 2015). The experimental setup is shown in Fig. 2.11 and other important details are given in Table 2.5.

A four-stroke, single-cylinder, spark ignition direct injection (SIDI) engine (four valves with pent-roof) was used in this study. The engine had a centrally mounted spark plug and side-mounted injector. More details about the engine modifications can be found in the original work (Peterson et al. 2015). Nd:YAG laser was used for toluene LIF excitation. Laser beam was formed into light sheet (0.5 mm thickness), which was reflected off by 45° mirror in the engine crankcase and then passed through the quartz-bottom piston, providing a vertical viewing plane within the central axis of the cylinder.

To avoid the quenching effect of oxygen in toluene fluorescence signals, high purity nitrogen was used as the intake gas during the engine operation. Some portion of nitrogen was sent to a bubbling seeder to add toluene vapour (2.75% w/w) in order

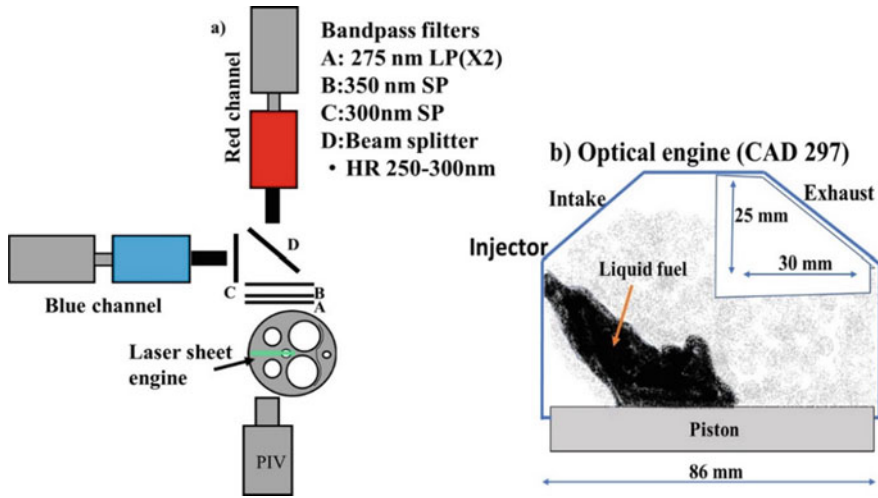


Fig. 2.11 Experimental setup of LIF investigations using high-speed toluene-LIF thermometry with two-colour detection scheme in a GDI engine

Table 2.5 Engine operating condition (Peterson et al. 2015)

Parameters	Value
Engine speed	1000 RPM
Injection timing	294–301° CA bTDC
Intake pressure and temperature	95 kPa, 295 K
Coolant temperature	333 K

to compare the time progression of in-cylinder temperature between motored- and combustion cycles. The area of interest for LIF temperature measurement is shown in Fig. 2.12. Small area marked by a rectangle was used for calibration of LIF signals with temperature. Signal ratio and calibrated temperature variations are shown in Fig. 2.13.

Temperature images were taken within $25 \times 30 \text{ mm}^2$ field-of-view to analyse temporal evolution of liquid droplet distribution, which revealed that the temperature stratification originally created by evaporative cooling and bulk-flow motion-driven mixing over time reduces the temperature gradients. A strong counter-clockwise vortex can be observed at 315° CA. The temperature decreased by $\sim 50 \text{ K}$ due to spray induced cooling. Low-temperature pocket can be spotted in the bottom right corner at 324° CA. This exhibited that the temperature inhomogeneity diminished well after the end of the injection. Thus, the injection timing can be instrumental in temperature stratification, however, a larger field of view and combustion imaging is required for deeper insights into the after-effects.

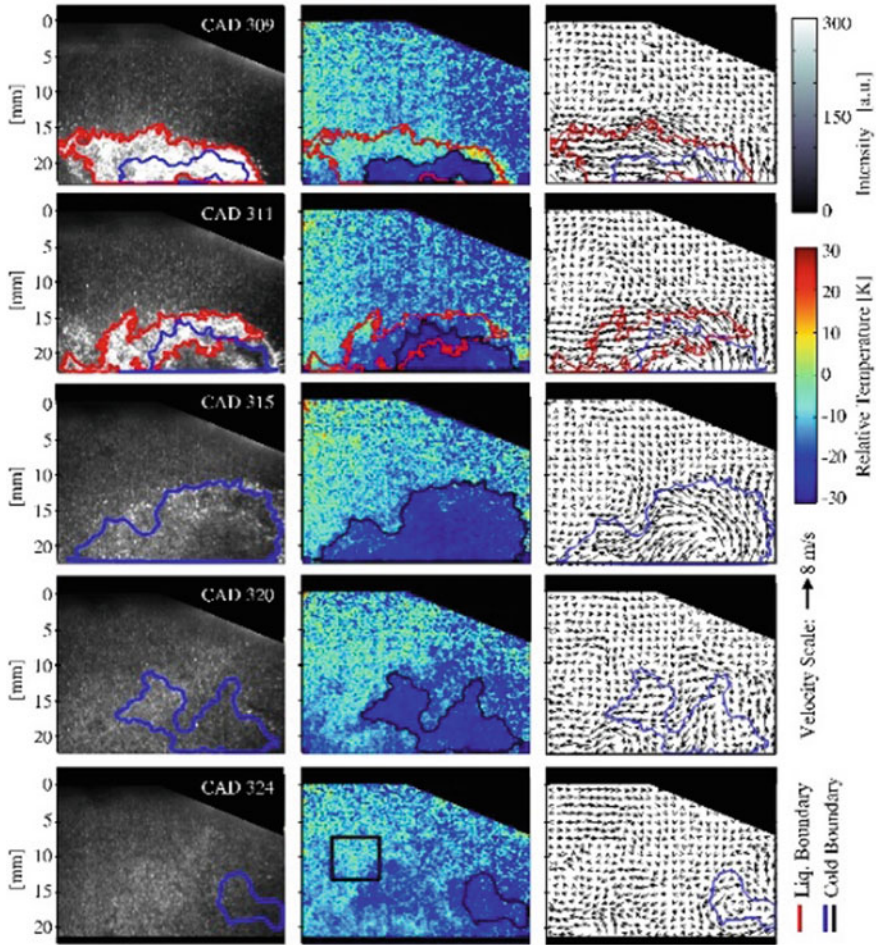
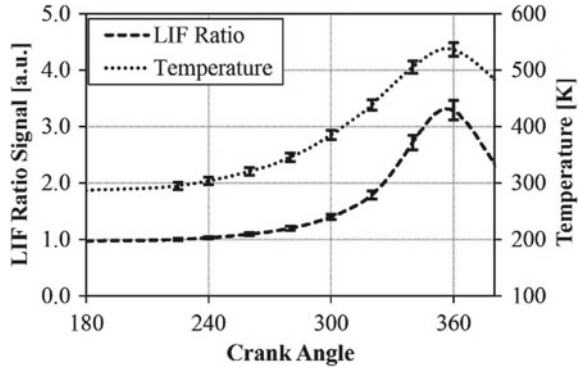


Fig. 2.12 Analysis of spray-induced thermal stratification with multiple optical diagnostics (Peterson et al. 2015)

2.4.4 A Case Study of Fuel Stratification in Reactivity Controlled Compression Ignition (RCCI) Combustion Engine by Optical Diagnostics

RCCI combustion is a promising low-temperature combustion (LTC) concept for expanding the limited operating window of LTC with simultaneously low emissions of soot and NO_x . Reactivity stratification due to low and high reactivity fuels is the key parameter to control the combustion in RCCI mode. Thus, advanced optical diagnostics of RCCI is required for simultaneous measurement of fuel and temperature stratification to analyze the effect of reactivity stratification at different engine

Fig. 2.13 Temperature and LIF ratio variations with crank angle (Peterson et al. 2015)



operating conditions. Tang et al. (2017) used toluene-PLIF to study fuel stratification in RCCI combustion engines. They used formaldehyde and OH-PLIF to investigate the low- and high-temperature heat releases.

A light-duty optical engine was modified to operate in RCCI mode combustion up to 7 bar IMEP. Iso-octane was introduced via port injection and n-heptane was injected late in the compression stroke via direct injection. Specifications of the engine are given in Table 2.6.

For providing optical access of the laser beam into the engine combustion chamber, a quartz rim covering 36 mm of the stroke length was installed. A 40-mm width slice was cut from the piston rim to enable the laser to pass into the piston bowl during combustion. Laser sheet was generated by a 10 Hz Nd:YAG laser. 30 mm wide and 0.8 mm thick laser sheet was adjusted to pass 10 mm below the fire-deck for successful analysis of early combustion events. A common Bowditch design was used for capturing the signals with the help of a 45° inclined mirror and an ICCD camera. The details of the piston design are given in Fig. 2.14.

Table 2.6 Engine specifications for optical diagnostics of RCCI combustion (Tang et al. 2017)

Engine type	4 stroke
Bore	92 mm
Stroke	100 mm
Displacement	0.66L
Connecting rod length	155 mm
Compression ratio	11
Combustion chamber shape	Cylindrical
Combustion chamber diameter	63 mm
DI pressure	600 bar
Holes number of DI injector	6
Spray included angle of DI injector	150°
Injector hole diameter of DI injector	0.15 mm

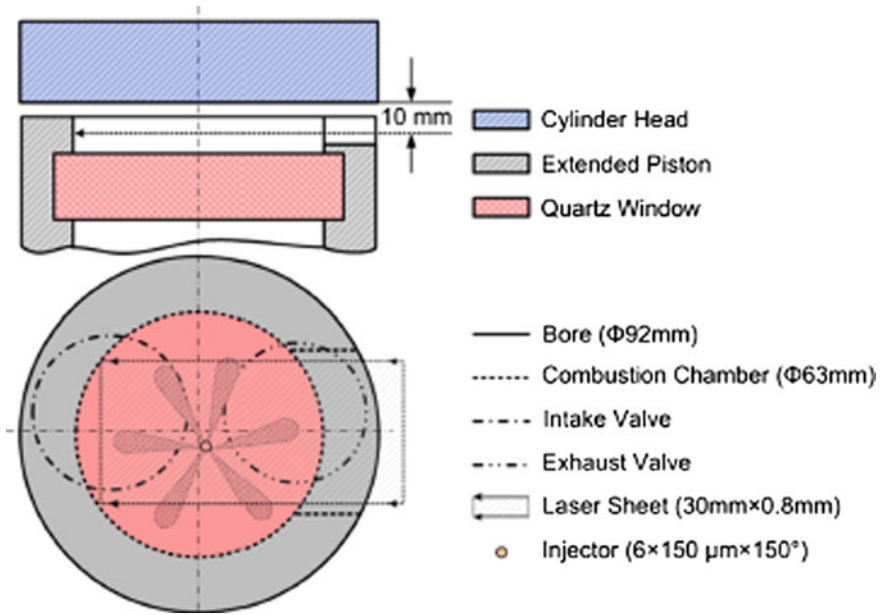


Fig. 2.14 Piston modifications for laser access in optical RCCI engine (Tang et al. 2017)

In this study, three different laser beams were used for excitation. First laser beam having 266 nm wavelength was used for toluene-PLIF under motored engine condition to study fuel stratification. Toluene (1% v/v) was used as tracer for both fuels. A 355-nm laser pulse was used for formaldehyde-PLIF to study the combustion events. An edge filter (390–480 nm) was employed for the formaldehyde signal acquisition. No PAH signals were detected, indicating low level of soot formation. 282.95 nm excitation was used for OH-PLIF with 308–325 nm edge filter. Engine operating conditions are given in Table 2.7. In Table 2.7, different RCCI combustion modes have been categorized as RCCI-xx, where xx represents the start of main injection timing.

Results from toluene-PLIF revealed that in case of RCCI-90, the fuel stratification was minimum. As ignition was retarded, the extent of stratification increased with more high reactive heptane near the combustion chamber wall. Maximum stratification was achieved by RCCI-10. The results of formaldehyde/OH PLIF are shown in Figs. 2.15 and 2.16. From Fig. 2.15, it can be observed that formaldehyde starts building-up much earlier in RCCI-90 compared to RCCI-25 and RCCI-10. This is well justified by the results of fuel stratification, which depicted the homogeneous distribution of heptane. Thus, the low-temperature heat release started relatively earlier with formaldehyde formation. Comparison of Figs. 2.15 and 2.16 shows that the formaldehyde disappeared at the locations, where OH formation is started. Formaldehyde was consumed as temperature increased and OH started

Table 2.7 Engine operating conditions for various PLIF experiments (Tang et al. 2017)

		RCCI-90	RCCI-25	RCCI-10
Engine speed (rpm)		1200		
Inlet air pressure (bar)		1		
Inlet air temperature (°C)		75		
Fuel injection pressure(bar)	Port	3		
	Direct	600		
Iso-octane (% vol)		70		
N-heptane (% vol)		30		
Start of port injection(°aTDC)		-300		
Start of direct injection (°aTDC)		-90	-25	-10
Global equivalence ratio		0.77		
Gross IMEP (bar)		7.0	6.8	6.9

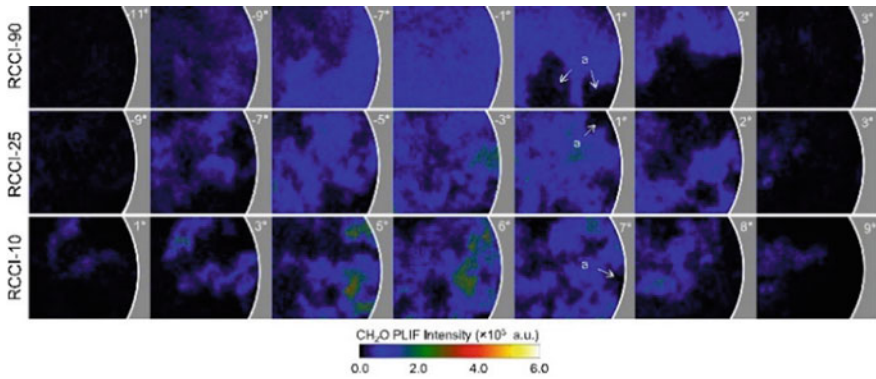


Fig. 2.15 PLIF image of formaldehyde (Tang et al. 2017)

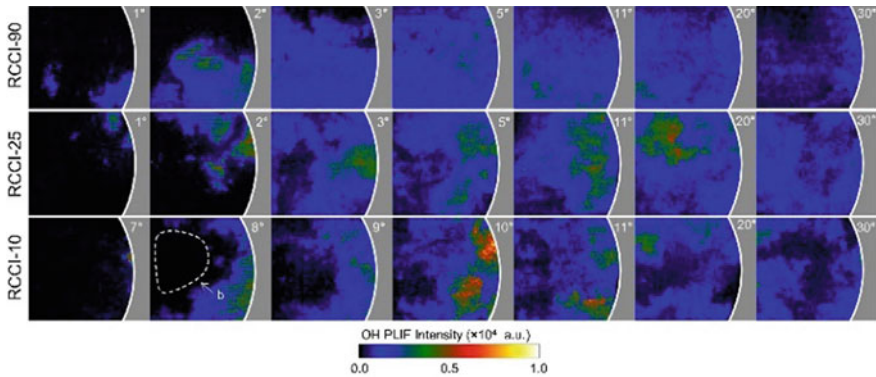


Fig. 2.16 OH PLIF images (Tang et al. 2017)

forming. Also, a higher concentration of OH can be observed near the cylinder walls for RCCI-10, which finally moved towards the centre. Combustion images also revealed that blue flames started at the periphery and auto-ignition occurred later at the center for RCCI-10. Therefore, a high degree of fuel stratification led to more controlled combustion. Retarded ignition timing increased control over combustion and extended high-temperature combustion to the centre of the bowl. This may result in a reduction in unburned HC emissions.

2.4.5 A Case Study of Flame Evolution in Gasoline Compression Ignition (GCI) Engine by LIF Technique

GCI is a novel LTC technique, in which low octane fuels can be used for achieving higher engine performance with lower emissions. Tang et al. (2017) employed multiple optical diagnostic techniques to understand the flame evolution in a light-duty optical engine operated in GCI mode (Fig. 2.17). Optical engine specifications

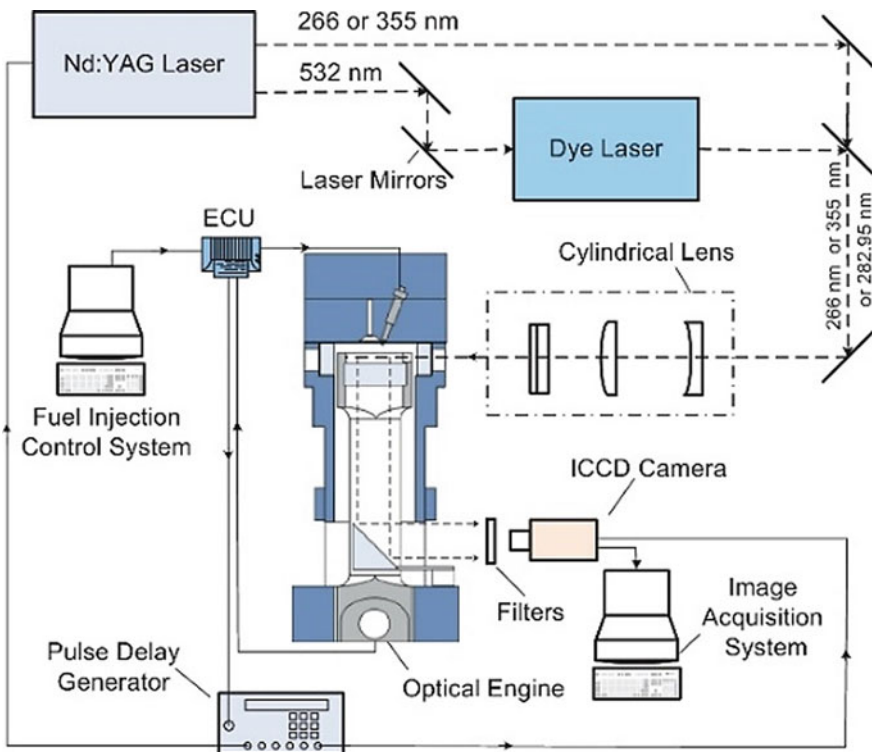


Fig. 2.17 Schematic of the optical setup in GCI optical engine (Tang et al. 2017)

Table 2.8 Optical GCI engine specifications (Tang et al. 2017)

Bore	92 mm
Stroke	100 mm
Displacement	0.664 L
Connecting rod length	155 mm
Compression ratio	11
Combustion chamber shape	Cylindrical
Combustion chamber diameter	63 mm
Common rail pressure	600 bar
Holes number for DI injector	6
Spray included angle	150°
Injector hole diameter	0.15 mm

Table 2.9 Engine operating conditions (Tang et al. 2017)

	PPC-25	PPC-90
Engine speed (rpm)	1200	–
Intake pressure (bar)	1	–
Intake temperature (°C)	125	–
DI pressure (bar)	600	–
Fuel	PRF70	–
Fuel mass (mg/cycle)	26	–
Direct injection (°ATDC)	–25	–90
Overall equivalence ratio	0.77	–
IMEP (bar)	5.99	5.90

are listed in Table 2.8. Table 2.9 depicts the details of engine operating conditions used in this study. In PPC-25 and PPC-90, the numbers indicate the main fuel injection timing. Single-injection strategy was adopted for both cases. The purpose of this investigation was to explore the fundamental combustion behaviour such as ignition, flame development, etc. in GCI combustion engines.

Investigations were carried out in a naturally aspirated, single-cylinder optical engine, in which Bowditch piston was used. An optical cylindrical combustion chamber was designed with a flat quartz window at the bottom, which provided optical access to the combustion chamber. A cut-out section of 40 mm was provided on the ring of the combustion chamber for the entry of the laser sheet into engine combustion chamber near TDC. A UV reflection mirror was mounted on the cylinder block. In this engine, modifications in the combustion chamber reduced the compression ratio to ~11 (Fig. 2.18).

A thin horizontal laser sheet (~1 mm thick, 30 mm wide) was produced by cylindrical lens group and then it was directed into the combustion chamber through the quartz ring window. The laser sheet was located in a plane 10 mm below the fire deck.

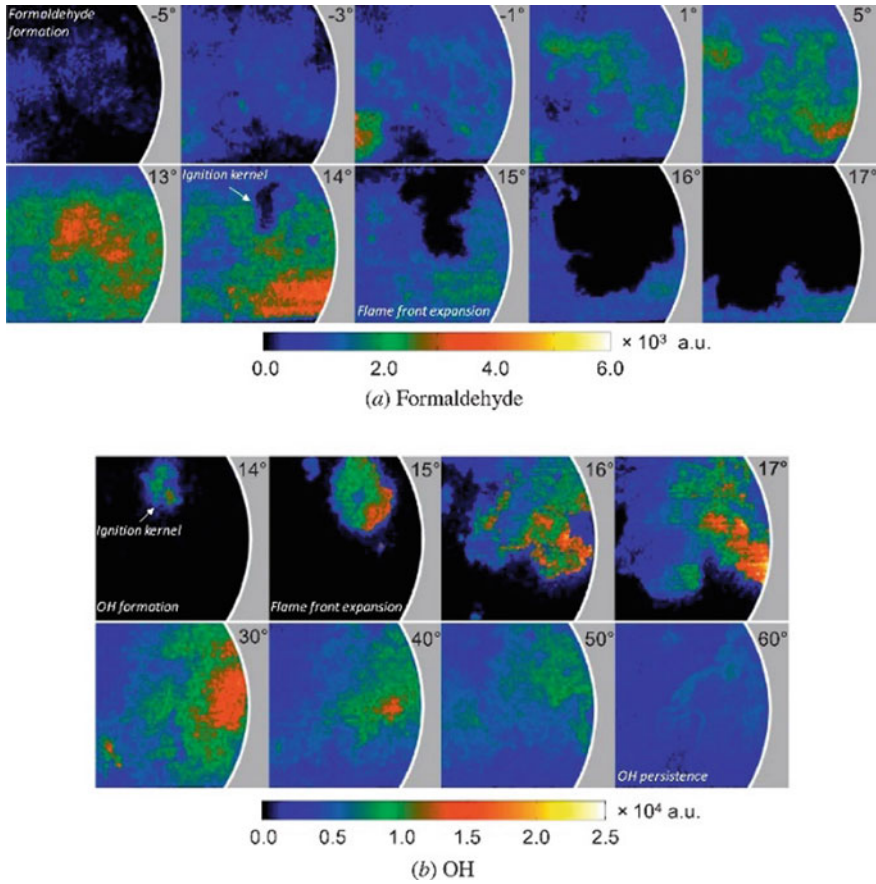


Fig. 2.18 Formaldehyde and OH PLIF for flame evolution in GCI engine (Tang et al. 2017)

For fuel tracer PLIF diagnostics, fourth harmonic Nd:YAG laser with 266 nm wavelength and 60 mJ/pulse energy was used for fuel tracer excitation. For formaldehyde and OH PLIF diagnostics, the third harmonic Nd:YAG laser with 355 nm wavelength and 70 mJ/pulse energy was used for formaldehyde excitation. For OH PLIF, the second harmonic of the Nd:YAG laser pumped dye laser, which generated a beam of 282.93 nm wavelength to excite $Q_1(6)$ line of the A-X (1, 0) transition of OH.

The results were divided into four stages:

- i. Multiple auto-ignition kernels emerging in the fuel-rich regions.
- ii. Flame front propagation of auto-ignition kernels towards fuel-lean regions.
- iii. Auto-ignition in the end-gas in fuel-lean regions.
- iv. A 'burnout' stage in the whole combustion chamber after the end of main heat release.

Formaldehyde LIF marks the low-temperature heat release at -5° bTDC. The distribution covers the entire combustion chamber by 13° aTDC. At 14° aTDC the flame kernel appears near the bowl periphery, much like conventional diesel combustion. OH LIF signal marks the start of high-temperature heat release, which then consumed the formaldehyde as combustion progressed. From this study, it was concluded that variations in the degree of fuel stratification caused by different fuel injection timings were responsible for this transformation in the flame development pattern in GCI engines.

2.4.6 A Case Study for Fuel Distribution in GDI Engine by LIF Technique

This study was focused on high-speed imaging to investigate the cycle-to-cycle variations and captured the rare events during HCCI combustion operated at a particular engine operating condition (Fig. 2.19).

In order to study the combustion behaviour of fuel within the cylinder, LIF technique was used in an optical gasoline direct injection (GDI) engine. In this study, hydroxyl radical LIF images were acquired in an optical square-piston engine.

For optical access (Fig. 2.20), laser A and laser B beams were directed into beam splitter, from where these laser beams were directed towards mirror M2. This beam was focused towards optical combustion chamber using various lenses, which made the combustion chamber optically accessible. In this study, crucial processes including the intake air-flow, mixture preparation, ignition, flame kernel growth,

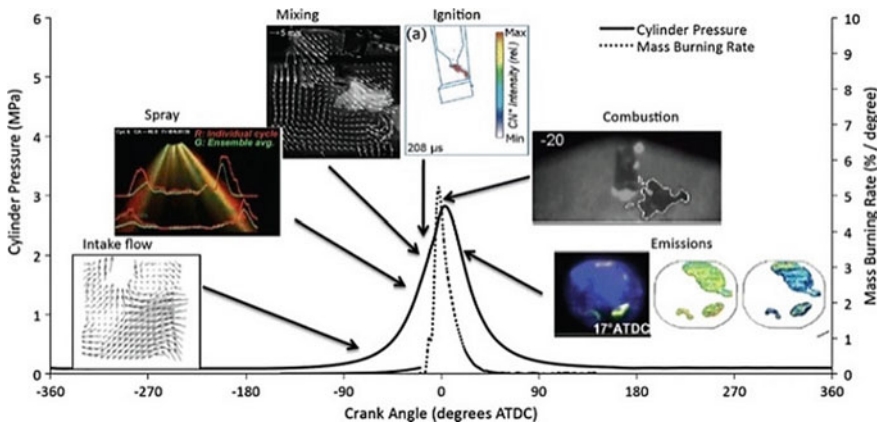


Fig. 2.19 The occurrence and timing of processes that were studied with high-speed imaging in SIDI engines are illustrated along with the in-cylinder pressure and mass-burn rate in a late injection SIDI engine experiment (Sick et al. 2010)

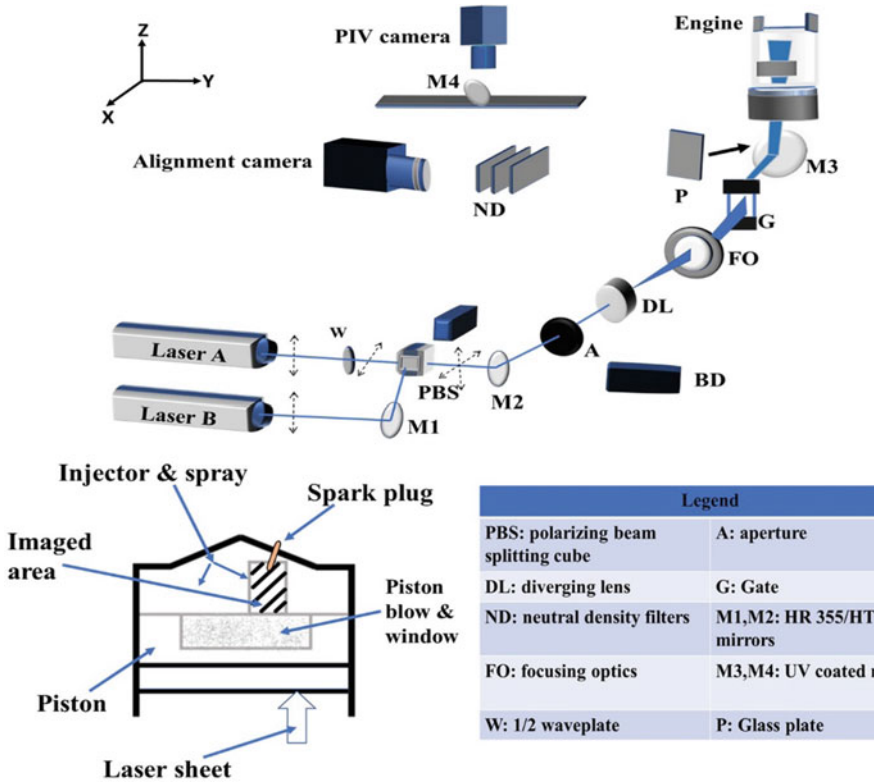


Fig. 2.20 Experimental setup

combustion, and pollutant formation during a cycle in the GDI engine were investigated. Equivalence ratio (ER) distribution was obtained by LIF. The results depicted that cycle averaged ER was significantly different from the individual cycle in the vicinity of spark plug. During the initial stage of spray, there were some similarities, however, as the cycle progressed, individual cycles showed that the mixture strength was below the combustible limit. This might lead to misfiring and cycle-to-cycle variations in a GDI engine. Also, the cycle averaged results of CFD model could be erroneous in predicting ideal parameters for GDI engine operation.

2.5 Summary

Laser-induced fluorescence (LIF) is a popular tool for state-of-the-art quantitative analysis of temperature and species distribution. Combustion researchers are putting significant efforts to make the fuel-air mixture further leaner. Under such a scenario, precise control of fuel-air mixture is important because local over-leaning may lead

to combustion failure, resulting in emission spikes. LIF can be effectively used to avoid the possibility of such incidents. In this chapter, the scope of LIF application in IC engines has been discussed. This chapter provides a brief information related to different aspects of LIF such as fundamentals, components of LIF setup, methodology, and applications. A brief discussion on the design of optical access for the experimental IC engines has been provided. In IC engines, LIF has been successfully implemented to investigate in situ temperature stratification and autoignition phenomenon during combustion. Various factors affecting LIF results have been also discussed, which showed that both, the temperature and pressure affect the accuracy of quantitative measurements using LIF. Several case studies related to the application of LIF in IC engines show the relevance of LIF technique for better realization of in-cylinder processes and combustion. Development of advanced and user-friendly commercial tools for LIF would help develop effective emission control technology for IC engines and improve the fuel economy.

References

- Banko AJ, Benson MJ, Gunady IE, Elkins CJ, Eaton JK (2020) An improved three-dimensional concentration measurement technique using magnetic resonance imaging. *Exp Fluids* 61(2):53
- Bardi M, Di Lella A, Bruneaux G (2019) A novel approach for quantitative measurements of preferential evaporation of fuel by means of two-tracer laser induced fluorescence. *Fuel* 239:521–533
- Bessler WG, Schulz C, Hartmann M, Schenk M (2001). Quantitative in-cylinder NO-LIF imaging in a direct-injected gasoline engine with exhaust gas recirculation. *SAE Trans* pp 1837–1846
- Bessler WG, Schulz C, Shin DI, Lee T, Jeffries JB, Hanson RK (2002) Strategies for NO laser-induced fluorescence in methane/air flames at pressures between 1 and 60 bar. In: *Laser applications to chemical and environmental analysis*, p FB4. Optical Society of America
- Brackmann C, Nygren J, Bai X, Li Z, Bladh H, Axelsson B, Denbratt I, Koopmans L, Bengtsson PE, Aldén M (2003) Laser-induced fluorescence of formaldehyde in combustion using third harmonic Nd: YAG laser excitation. *Spect Acta Part A Mol Biomol Spectrosc* 59(14):3347–3356
- Burkert A, Triebel W, Stafast H, König J (2002) Single-shot imaging of gas temperatures in low-temperature combustion based on laser-induced fluorescence of formaldehyde. *Proc Combust Inst* 29(2):2645–2651
- Burkert A, Paa W, Reimert M, Klinkov K, Eigenbrod C (2013) Formaldehyde LIF detection with background subtraction around single igniting GTL diesel droplets. *Fuel* 111:384–392
- Chen B, Feng L, Wang Y, Ma T, Liu H, Geng C, Yao M (2019) Spray and flame characteristics of wall-impinging diesel fuel spray at different wall temperatures and ambient pressures in a constant volume combustion vessel. *Fuel* 235:416–425
- Cheong J, Wigger S, Füller HJ, Kaiser SA (2020) High-resolution LIF-Imaging of the oil film thickness in the piston-ring/cylinder-liner contact in an optical tribometer. *Tribol Int* 106230
- Cordier M, Itani L, Bruneaux G (2020) Quantitative measurements of preferential evaporation effects of multi-component gasoline fuel sprays at ECN Spray G conditions. *Int J Engine Res* 21(1):185–198
- Deschamps BM, Smallwood GJ, Prieur J, Snelling DR, Gülder ÖL (1996) Surface density measurements of turbulent premixed flames in a spark-ignition engine and a Bunsen-type burner using planar laser-induced fluorescence. In: *Symposium (international) on combustion*, vol 26, no 1, pp 427–435. Elsevier

- Donkerbroek AJ, Van Vliet AP, Somers LMT, Frijters PJM, Klein-Douwel RJH, Dam NJ, Meerts WL, ter Meulen JJ (2010) Time-and space-resolved quantitative LIF measurements of formaldehyde in a heavy-duty diesel engine. *Combust Flame* 157(1):155–166
- Fujikawa T, Fukui K, Hattori Y, Akihama K (2006) 2-D temperature measurements of unburned gas mixture in an engine by two-line excitation LIF technique. SAE technical paper 2006-01-3336
- Gamba M, Miller VA, Mungal MG, Hanson RK (2015) Temperature and number density measurement in non-uniform supersonic flow fields undergoing mixing using toluene PLIF thermometry. *Appl Phys B* 120(2):285–304
- Gessenhardt C, Schulz C, Kaiser SA (2015) Endoscopic temperature imaging in a four-cylinder IC engine via two-color toluene fluorescence. *Proc Combust Inst* 35(3):3697–3705
- Haessler H, Bockhorn H, Pfeifer C, Kuhn D (2012) Formaldehyde-LIF of dimethyl ether during auto-ignition at elevated pressures. *Flow Turbul Combust* 89(2):249–259
- Hildingsson L, Johansson B, Hultqvist A, Särner G, Richter M, Aldén M (2005) Simultaneous formaldehyde and fuel-tracer LIF imaging in a high-speed diesel engine with optically accessible realistic combustion chamber. SAE Technical Paper 2005-24-008
- Itani LM, Bruneaux G, Di Lella A, Schulz C (2015) Two-tracer LIF imaging of preferential evaporation of multi-component gasoline fuel sprays under engine conditions. *Proc Combust Inst* 35(3):2915–2922
- Kaiser SA, Schild M, Schulz C (2013) Thermal stratification in an internal combustion engine due to wall heat transfer measured by laser-induced fluorescence. *Proc Combust Inst* 34(2):2911–2919
- Koban W, Koch JD, Hanson RK, Schulz C (2004) Absorption and fluorescence of toluene vapor at elevated temperatures. *Phys Chem Chem Phys* 6(11):2940–2945
- Krämer H, Einecke S, Schulz C, Sick V, Natrass SR, Kitching JS (1998). Simultaneous mapping of the distribution of different fuel volatility classes using tracer-LIF tomography in an IC engine. SAE Trans 1049–1060
- Kranz P, Kaiser SA (2019) LIF-based imaging of preferential evaporation of a multi-component gasoline surrogate in a direct-injection engine. *Proc Combust Inst* 37(2):1365–1372
- Lachaux T, Musculus MP (2007) In-cylinder unburned hydrocarbon visualization during low-temperature compression-ignition engine combustion using formaldehyde PLIF. *Proc Combust Inst* 31(2):2921–2929
- Li Y, Zhao H, Ma T (2006) Flow and mixture optimization for a fuel stratification engine using PIV and PLIF techniques. *J Phys Conf Ser* 45(1):59. IOP Publishing
- Li B, Jonsson M, Algotsson M, Bood J, Li ZS, Johansson O, Aldén M, Tunér M, Johansson B (2013) Quantitative detection of hydrogen peroxide in an HCCI engine using photo fragmentation laser-induced fluorescence. *Proc Combust Inst* 34(2):3573–3581
- Li B, Zhang D, Yao M, Li Z (2017) Strategy for single-shot CH₃ imaging in premixed methane/air flames using photofragmentation laser-induced fluorescence. *Proc Combust Inst* 36(3):4487–4495
- Lind S, Trost J, Zigan L, Leipertz A, Will S (2015) Application of the tracer combination TEA/acetone for multi-parameter laser-induced fluorescence measurements in IC engines with exhaust gas recirculation. *Proc Combust Inst* 35(3):3783–3791
- Lind S, Retzer U, Will S, Zigan L (2017) Investigation of mixture formation in a diesel spray by tracer-based laser-induced fluorescence using 1-methylnaphthalene. *Proc Combust Inst* 36(3):4497–4504
- Ma X, Xu H, Jiang C, Shuai S (2014) Ultra-high speed imaging and OH-LIF study of DMF and MF combustion in a DISI optical engine. *Appl Energy* 122:247–260
- Ma L, Lei Q, Ikeda J, Xu W, Wu Y, Carter CD (2017) Single-shot 3D flame diagnostic based on volumetric laser induced fluorescence (VLIF). *Proc Combust Inst* 36(3):4575–4583
- Malmqvist E, Jonsson M, Larsson K, Aldén M, Bood J (2016) Two-dimensional OH-thermometry in reacting flows using photofragmentation laser-induced fluorescence. *Combust Flame* 169:297–306
- Miles PC (2014) The history and evolution of optically accessible research engines and their impact on our understanding of engine combustion. In: ASME 2014 internal combustion engine division fall technical conference. American Society of Mechanical Engineers Digital Collection

- Nygren J, Hult J, Richter M, Aldén M, Christensen M, Hultqvist A, Johansson B (2002) Three-dimensional laser induced fluorescence of fuel distributions in an HCCI engine. *Proc Combust Inst* 29(1):679–685
- Omar M, Dominique T, Patrizio M, Jérôme B (2020) Investigation on the conditions leading to the micro-explosion of emulsified fuel droplet using two colors LIF method. *Exper Thermal Fluid Sci* 110106
- Ottenwälder T, Schulz C, Raffius T, Koß HJ, Grünefeld G, Heufer KA, Pischinger S (2018) Quantitative nitrogen oxide measurements by laser-induced fluorescence in diesel-like n-heptane jets with enhanced premixing. *Combust Flame* 188:250–261
- Peterson B, Baum E, Böhm B, Sick V, Dreizler A (2013) High-speed PIV and LIF imaging of temperature stratification in an internal combustion engine. *Proc Combust Inst* 34(2):3653–3660
- Peterson B, Baum E, Böhm B, Sick V, Dreizler A (2014) Evaluation of toluene LIF thermometry detection strategies applied in an internal combustion engine. *Appl Phys B* 117(1):151–175
- Peterson B, Baum E, Böhm B, Sick V, Dreizler A (2015) Spray-induced temperature stratification dynamics in a gasoline direct-injection engine. *Proc Combust Inst* 35(3):2923–2931
- Peterson B, Baum E, Dreizler A, Böhm B (2019) An experimental study of the detailed flame transport in a SI engine using simultaneous dual-plane OH-LIF and stereoscopic PIV. *Combust Flame* 202:16–32
- Qin S, Krohn B, Petrov V, Manera A (2020) Velocity and scalar fields of a turbulent buoyant jet in the self-similar region. *Nucl Technol* 206(2):307–321
- Raman V, Tang Q, An Y, Shi H, Sharma P, Magnotti G, Chang J, Johansson B (2020) Impact of spray-wall interaction on the in-cylinder spatial unburned hydrocarbon distribution of a gasoline partially premixed combustion engine. *Combust Flame* 215:157–168
- Schießl R, Maas U (2003) Analysis of end gas temperature fluctuations in an SI engine by laser-induced fluorescence. *Combust Flame* 133(1–2):19–27
- Schmitt S, Wick M, Wouters C, Ruwe L, Graf I, Andert J, Hansen N, Pischinger S, Kohse-Höinghaus K (2020) Effects of water addition on the combustion of iso-octane investigated in laminar flames, low-temperature reactors, and an HCCI engine. *Combust Flame* 212:433–447
- Schrewe MR, Ghandhi JB (2007) Near-wall formaldehyde planar laser-induced fluorescence measurements during HCCI combustion. *Proc Combust Inst* 31(2):2871–2878
- Schulz C, Sick V (2005) Tracer-LIF diagnostics: quantitative measurement of fuel concentration, temperature and fuel/air ratio in practical combustion systems. *Prog Energy Combust Sci* 31(1):75–121
- Schulz C, Yip B, Sick V, Wolfrum J (1995) A laser-induced fluorescence scheme for imaging nitric oxide in engines. *Chem Phys Lett* 242(3):259–264
- Scott B, Willman C, Williams B, Ewart P, Stone R, Richardson D (2017) In-cylinder temperature measurements using laser induced grating spectroscopy and two-colour PLIF. *SAE Int J Engines* 10(4):2191–2201
- Shen X, Gao X, Li Z, Li B, Zheng C, Sun Z, Ni M, Cen K, Aldén M (2012) PLIF diagnostics of NO oxidization and OH consumption in pulsed corona discharge. *Fuel* 102:729–736
- Shi H, Tang Q, An Y, Raman V, Sim J, Chang J, Magnotti G, Johansson B (2020) Study of spray/wall interaction in transition zones from HCCI via PPC to CI combustion modes. *Fuel* 268:
- Shibata G, Nishiuchi S, Xie P, Takai S, Ogawa H, Kobashi Y (2020) Measurements of fuel adhesion on cylinder walls and fuel wall-flow behavior with post diesel fuel injections. *Int J Engine Res* 21(2):352–366
- Sick V, Drake MC, Fansler TD (2010) High-speed imaging for direct-injection gasoline engine research and development. *Exp Fluids* 49(4):937–947
- Strozzi C, Claverie A, Prevost V, Sotton J, Bellenoue M (2019) HCCI and SICI combustion modes analysis with simultaneous PLIF imaging of formaldehyde and high-speed chemiluminescence in a rapid compression machine. *Combust Flame* 202:58–77
- Tang Q, Liu H, Li M, Geng C, Yao M (2017a) Multiple optical diagnostics on effect of fuel stratification degree on reactivity controlled compression ignition. *Fuel* 202:688–698

- Tang Q, Liu H, Li M, Yao M, Li Z (2017b) Study on ignition and flame development in gasoline partially premixed combustion using multiple optical diagnostics. *Combust Flame* 177:98–108
- Tang Q, Liu H, Ran X, Li M, Yao M (2020) Effects of direct-injection fuel types and proportion on late-injection reactivity controlled compression ignition. *Combust Flame* 211:445–455
- Thurber MC (1999) Acetone Laser-induced fluorescence for temperature and multi parameter imaging in gaseous flows. PhD thesis, Stanford University
- Tran KH, Guibert P, Morin C, Bonnet J, Pounkin S, Legros G (2015) Temperature measurements in a rapid compression machine using anisole planar laser-induced fluorescence. *Combust Flame* 162(10):3960–3970
- Verbiezen K, Klein-Douwel RJH, Van Vliet AP, Donkerbroek AJ, Meerts WL, Dam NJ, Ter Meulen JJ (2007) Quantitative laser-induced fluorescence measurements of nitric oxide in a heavy-duty Diesel engine. *Proc Combust Inst* 31(1):765–773
- Williams B, Ewart P, Wang X, Stone R, Ma H, Walmsley H, Cracknell R, Stevens R, Richardson D, Fu H, Wallace S (2010) Quantitative planar laser-induced fluorescence imaging of multi-component fuel/air mixing in a firing gasoline-direct-injection engine: effects of residual exhaust gas on quantitative PLIF. *Combust Flame* 157(10):1866–1878
- Wu Y, Xu W, Lei Q, Ma L (2015) Single-shot volumetric laser induced fluorescence (VLIF) measurements in turbulent flows seeded with iodine. *Opt Express* 23(26):33408–33418
- Zabeti S, Drakon A, Faust S, Dreier T, Welz O, Fikri M, Schulz C (2015) Temporally and spectrally resolved UV absorption and laser-induced fluorescence measurements during the pyrolysis of toluene behind reflected shock waves. *Appl Phys B* 118(2):295–307
- Zhang Z, Li T, Shi W (2019a) Ambient Tracer-LIF for 2-D quantitative measurement of fuel concentration in gas jets. *Energy* 171:372–384
- Zhang Q, Su J, Du W, Yuan H, Yang F, Tan S (2019b) Experimental study on mixing phenomenon inside reactor down-comer under single-loop injection using laser induced fluorescence. *Prog Nucl Energy* 117:
- Zhao H, Peng Z, Ma T (2004) Investigation of the HCCI/CAI combustion process by 2-D PLIF imaging of formaldehyde. SAE technical paper 2004-01-1901